

The Role of Projectile Configuration and Viscosity on the Launch Dynamics of Supersonic Projectiles

C.K.Muthukumaran¹

Department of Aerospace, Indian Institute of Space Science and Technology, Trivandrum, Kerala-695547

G.Rajesh^{2†}

Dept. of Mechanical and Automotive Engineering, Keimyung University, 1000 Shindang Dong, Dalseo-Gu, Daegu-704-701, SOUTH KOREA

rajesh@kmu.ac.kr

H D Kim³

School of Mechanical Engineering, Andong National University, SOUTH KOREA,

The aerodynamics of a projectile launched from barrels of various devices is quite complicated due to its interactions with the unsteady flow field around it. A computational study using moving grid method is performed here to analyze the effect of the projectile-shock wave interaction. Cylindrical and conical projectiles have been employed to study such interactions and the fluid dynamics of such flow fields. It is found that the overall effect of projectile overtaking a blast wave on the unsteady aerodynamic characteristics of the projectile is hardly affected by the projectile configurations. However, it is noticed that the projectile configurations do affect the unsteady flow structures and hence the drag coefficient for the conical projectile shows considerable variation from that of the cylindrical projectile. The projectile aerodynamic characteristics, when it interacts with the secondary shock wave, are analyzed in detail. It is also observed that the change in the characteristics of the secondary shock wave during the interaction is different for different projectile configurations. Both inviscid and viscous simulations were done to study the projectile aerodynamics. It is found that the effect of the viscosity on the projectile aerodynamics is negligible but the viscosity does affect the unsteady flow structures around the projectile.

¹ *Research Scholar, Department of Aerospace, Indian Institute of Space Science and Technology, Trivandrum, Kerala-695547*

^{2†} *Corresponding Author, Assistant Professor, Dept. of Mechanical and Automotive Engineering, Keimyung University, 1095 Dalgubeoldaerom Dalseo-Gu, Daegu 704-701, SOUTH KOREA.*

³ *Professor, School of Mechanical Engineering, Andong National University, SOUTH KOREA,*

Nomenclature

A	=	Projected frontal area of the projectiles
a	=	Speed of sound, m/s
C_d	=	Coefficient of drag
D	=	Drag force, N
M	=	Mach number
M_{p1}	=	Projectile Mach number relative to still air
M_{p2}	=	Projectile Mach number relative to flow behind the moving shock wave
M_s	=	Shock wave Mach number
P	=	Pressure, N/m^2
t	=	time, ms
u	=	Velocity, m/s
ρ	=	Density, kg/m^3
Subscript		
P	=	Projectile
S	=	Shock wave
1,2	=	Downstream and upstream of the moving shock wave

I. Introduction

The unsteady flow fields induced by the projectile when it is launched from a barrel attracted attention of many researchers since it involve various complicated fluid dynamic processes associated with its motion¹⁻⁵. The primary flow disturbances which make the flow field quite unsteady and complex are the flow interfaces and interactions. On the other hand, there are projectile flow-field interactions which affect the flight stability of the moving projectile in the flow field. One of the major interactions is the projectile blast wave interaction when the projectile catches up the primary blast wave and overtakes it. Later the flow field becomes more complicated when the secondary blast wave overtakes the projectile and interacts with the primary blast wave. These consecutive interactions lead to the projectile overtaking problem which has the significant influence on the unsteady aerodynamics characteristics of the projectiles in such flow fields.

Takayama and Jiang⁶ have done a computational analysis to study the fluid dynamics of a moving projectile in an unsteady flow field. They noticed that the interaction between primary blast wave and bow shock wave generated due to the projectile movement in the unsteady flow field, strongly dependent on the projectile speed. Though the fluid dynamics of the flow field was fairly explained in their work, the aerodynamics associated with the flying projectile in the near field has not been addressed. Later, Jiang⁷ studied the effect of friction between the projectile wall and the launch tube wall on the wave dynamic processes. He concluded from his numerical results that when the pressure behind the projectile is higher, not only leading shock of the second blast overtakes the projectile, but the gas behind the projectile does so, which results in complex wave dynamic processes. He also found that there is a significant increase in the acceleration of the projectile due to this high pressure. Watanabe⁸ studied the fluid dynamics associated with the projectile overtaking problem. They used the one-dimensional theory to analyze the various overtaking criteria. They argued that the possible overtaking can be either subsonic or supersonic, depending on projectile relative Mach number. A computational study on the projectile overtaking a blast wave was performed by Rajesh et al⁹. Their results show that the projectile flow field cannot be categorized based on the relative projectile Mach number as the Mach number of the blast wave is continuously changing. It is also shown that the aerodynamic characteristics of the projectile are hardly affected by the overtaking process for smaller blast wave Mach numbers as the blast wave will become weak by the time it is overtaken by the projectile. They noticed that the projectile drag coefficient is greatly affected by the unsteady flow structures than the overtaking process. There have been studies on the interaction of various shaped projectiles with the flow fields. Bryson and Gross¹⁰ investigated the interaction of the strong shocks by solid objects of various shapes like cones, cylinders and the spheres in steady flow fields. They found that their experimental results have good agreement with the diffraction theory proposed by Whithams¹¹. Their experiments showed that the cylinders and the spheres qualitatively have the same kind of interaction pattern. The computations carried out so far have mainly been inviscid which could hardly capture the actual fluid dynamics of such flow fields. For example, the vorticity production during the shock wave diffraction at the exit of the launch tube cannot be obtained in the inviscid analysis. Also, there are slip-lines present in the flow field which cause shear layer growth. Moreover, the shock wave boundary layer interaction is of great importance in such flow fields which significantly affects the projectile aerodynamic characteristics. Some viscous simulations have been done by Ahmadakia and Shirani¹² to study the axisymmetric projectile overtaking problem at transonic and supersonic conditions by solving full Navier-Stokes equation with Baldwin-Lomax algebraic

turbulence models. Their results show that during the time the projectile overtakes the moving shock wave, the drag force decreases and even becomes negative possibly due to the pressure difference across the shock wave. They also observed that the pressure distribution on the projectile changes when the projectile overtakes the moving shock.

In the experiments conducted by Sun and Takayama,³ it is observable that the viscosity does not affect either the shock structure or the threshold value of the initial blast wave Mach number for the shock diffraction to occur. However, viscosity does affect the structure of the slip lines and the flow field near the wall. This work is hence aimed at capturing the fluid dynamics and aerodynamics of the unsteady projectile flow field interactions in the near field of a launch tube. Two projectile configurations have been employed to study this launch dynamics. A moving grid method is employed to computationally simulate the flow fields. The computations have been performed for various projectile and blast wave Mach numbers. Both inviscid and viscous simulations have been carried out to depict the real flow field features in the vicinity of the launch tube.

II. Computational Methodology

The computational study has been performed using a commercial software CFD-FASTRAN, which makes use of density-based finite volume method that solves the two-dimensional axi-symmetric Euler equations for Inviscid simulation. For viscous simulation, the Navier-Stokes equation with appropriate turbulence modelling is chosen. The *k-Epsilon* model is used to model the turbulence. It employs chimera mesh scheme for the structured grids. For simulating the projectile motion, the chimera mesh scheme allows the overlapping of one zone over the other. The communication between the chimera cells and the overlapping cells is established through a trilinear interpolation. The projectile is identified as the moving body with six degrees of freedom. The projectile motion is modeled with Euler's equations of motion which is numerically solved at every time step and it requires the physical information of the projectile such as mass, moment of inertia.

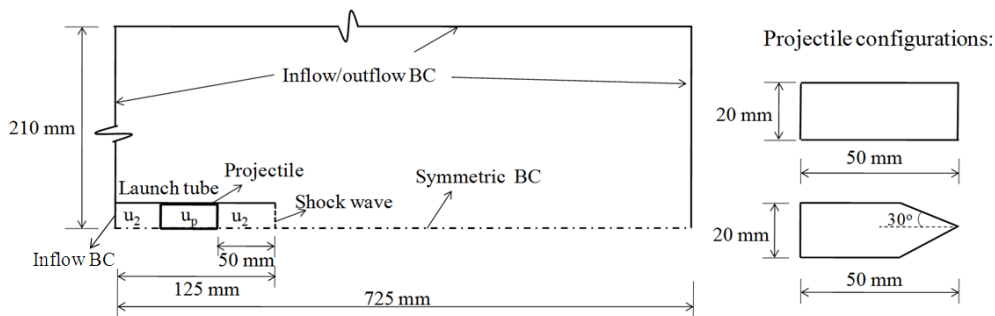


Figure 1: Computational domain, boundary conditions and Projectile configurations.

II.A. Computational methodology and boundary conditions

The computational domain, the boundary condition and the configuration of the projectile for the present study are illustrated in Fig. 1. The projectile has a length of 50 mm, diameter of 20 mm and the half-cone angle for the conical projectile is 30° . The computational domain and the conditions that are used here is same as that used by Rajesh and Kim⁹. The validation of the computational results can be found in Rajesh and Kim⁹.

The solver uses Van Leer's flux vector splitting scheme for spatial discretization which is of first order accuracy. The spatial accuracy of the scheme is increased to higher orders with the use of Osher-Chakravarthy flux limiter¹³. The time integration is carried out using point Jacobi fully implicit scheme.

The Inflow/outflow boundary is used which it is suitable for representing far-field boundary condition for external flow problem. Initially the projectile is given a velocity of M_{p1} , the flow ahead and behind the projectile is same as that of the projectile. Based on the velocity of the shock and the upstream conditions, the downstream flow conditions were given. When the computation starts, the moving shock wave is assumed at the exit of the launch tube in which the projectile is kept inside at a distance of 50 mm behind the shock wave. The flows ahead and behind the projectile are assumed to be in the same condition as that of the flow behind the moving shock wave that is at the exit of the launch tube, and the projectile also is moving with the velocity of the flow behind the moving shock wave.

The inlet boundary condition of the launch tube is same as that of the flow condition behind the projectile. The Inflow/outflow boundary is used which is suitable for representing far-field boundary condition for external flow problem. The inflow/outflow boundary condition is given at all the boundaries outside of the launch tube. The overset boundary conditions are given to the interface boundaries between chimera mesh and the overlapping mesh. The wall boundary conditions are given to the launch tube walls and the walls of the projectile wall.

II.B. Grid and time independence study

To determine the optimum mesh size and the time step size, the grid and time independence study has been performed for the viscous case as shown in Fig. 2. For inviscid case, the same grid system and time step as that of Rajesh et al were employed.⁹ For the viscous analysis, the grid independence study has been performed for the number of cells of 450000, 300000 and 150000 for the case of $M_{p1}=1.25$. The time independence study was performed with the time step of $2e-9$, $3.5e-9$ and $6.5e-9$ for the case of $M_{p1}=1.25$. The acceleration history of the

projectile is plotted for various time steps in Fig.2a. There are hardly any variations in the plots. Hence, for lower blast wave Mach numbers, the time step chosen was 3.5×10^{-9} and for higher Mach number the chosen time step was 2×10^{-9} . This is to assure the stability of the flow solver which is found to become worse when higher Mach numbers are chosen.

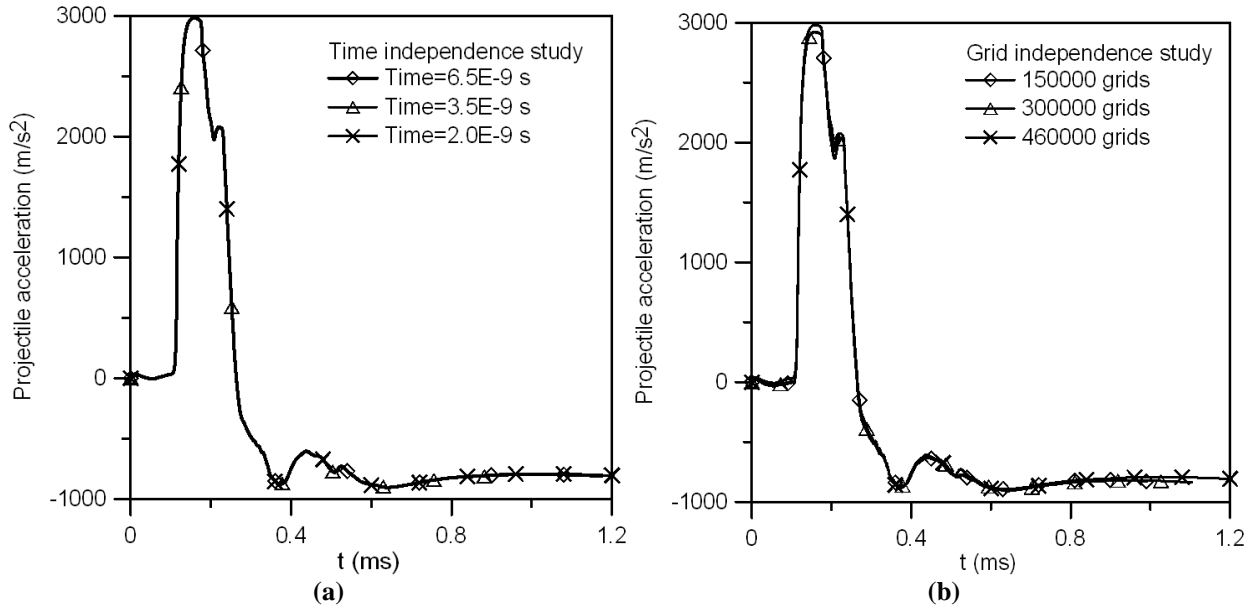


Figure 2: a: Time independence study b: Grid independence study.

III. Results and discussions

III.A. Aerodynamic characteristics -Inviscid flow

The acceleration history of the cylindrical and the conical projectile for both the inviscid and viscous cases are analyzed for various Mach numbers ranging from $M_s=1.4$ to $M_s=3.0$. Figures 4a, 3a, 5a and 6a show the acceleration histories of the projectiles for different Mach numbers. The acceleration history of the cylindrical projectile passing through unsteady flow structures for various Mach numbers is discussed for the inviscid case in Rajesh et al⁹.

Various state points are marked in the Fig. 3 based on the projectile-flow field interactions. The acceleration histories are nearly the same for both the cylindrical and conical projectiles for the Mach number investigated. Once the head of the projectile comes out of the launch tube, the front face of the projectile starts interacting with the low pressure under expanded jet resulting in pressure difference in the either side of the projectile. This causes the acceleration of the projectile from state a onwards, as shown in Fig. 3. The acceleration of the projectile continues till it interacts with the secondary shock wave which is marked as state b. From the Figures. 3, 4 and 5, it can be

seen that cases $M=3.0$, $M=2.5$, $M=2.0$ show similar trends in acceleration histories till the state b. At state b, there is a sudden drop in the acceleration is observed. This is the point, where the projectile interacts with the secondary shock wave and enters a flow field, where the relative Mach number becomes supersonic. From the state c to d,

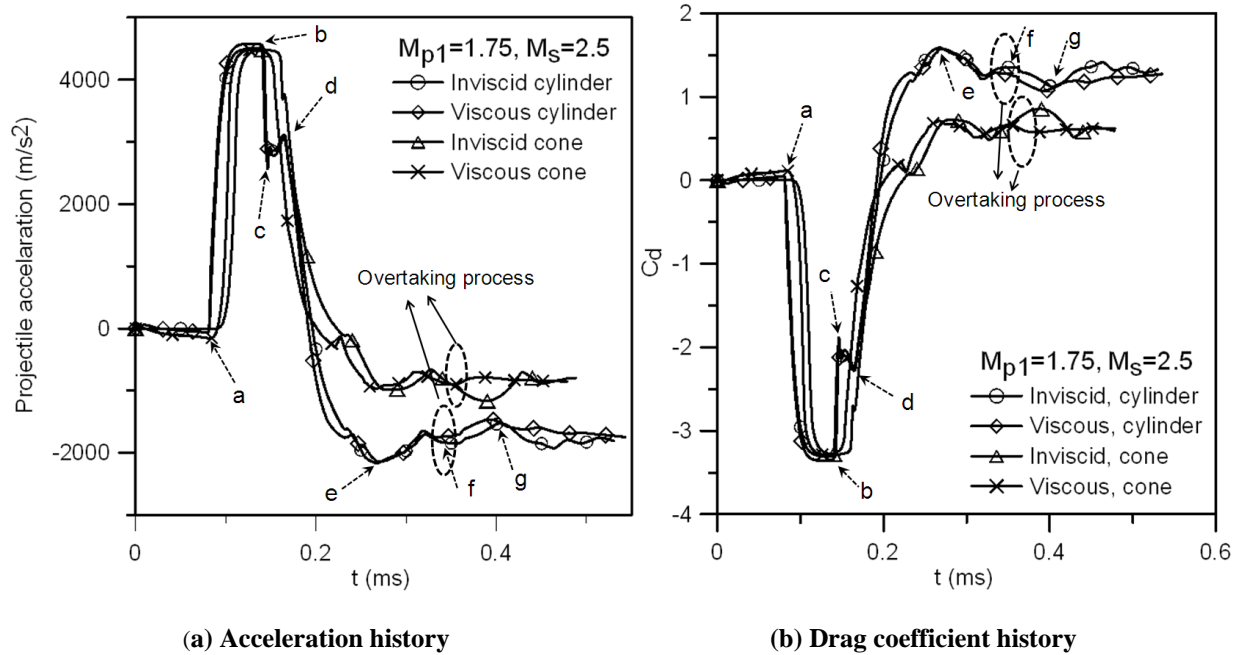


Figure 3: Acceleration and drag coefficient history of the cylindrical and conical projectile of inviscid and viscous simulation for Mach number $M_s=2.5$ and $M_{p1}=1.75$.

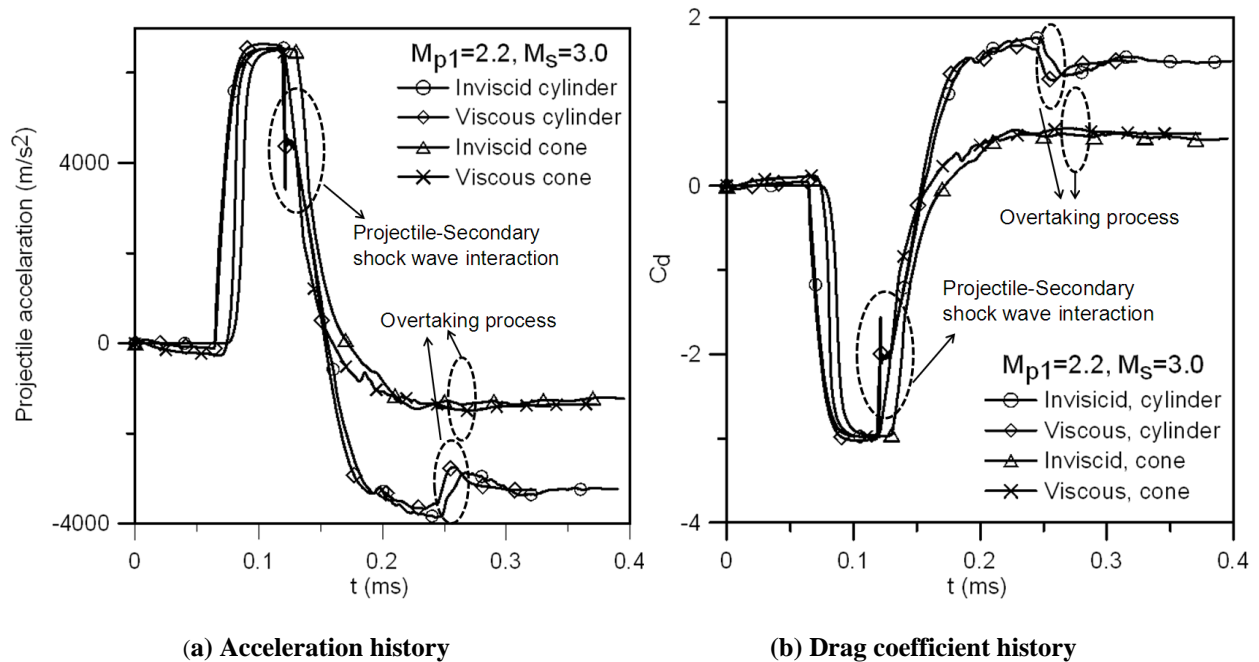


Figure 4: Acceleration and drag coefficient history of the cylindrical and conical projectile of inviscid and viscous simulation for Mach number $M_s=3.0$ and $M_{p1}=2.2$.

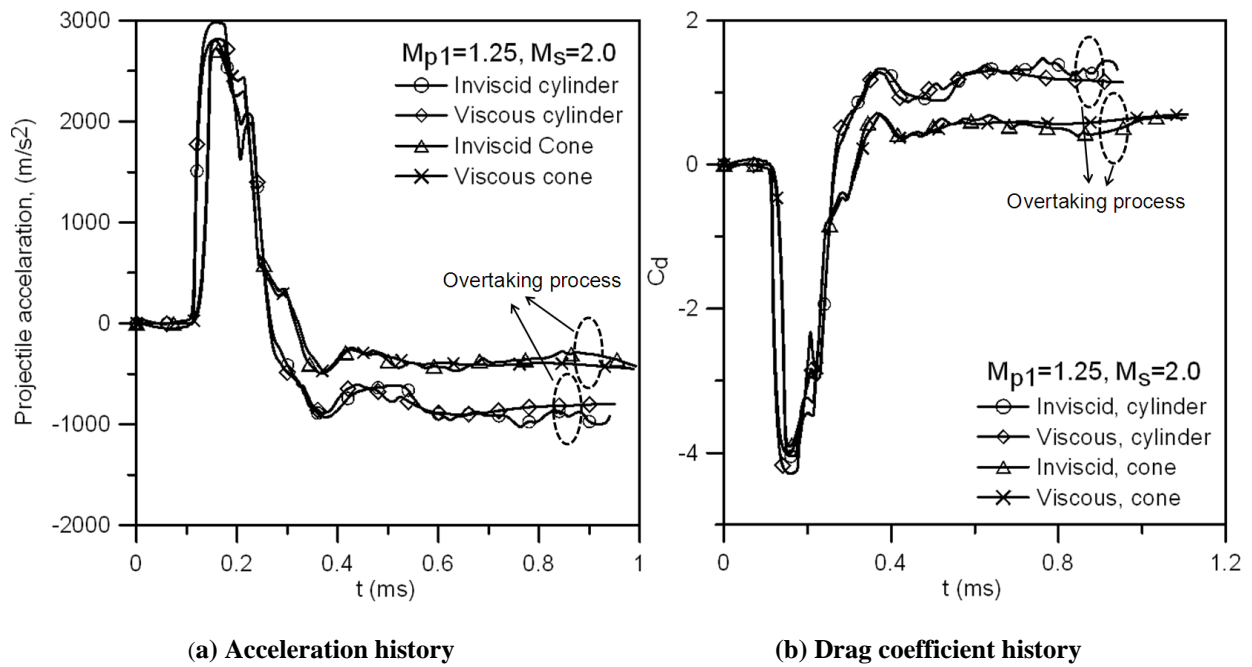


Figure 5: Acceleration and drag coefficient history of the cylindrical and conical projectile of inviscid and viscous simulation for Mach number $M_s=2.0$ and $M_{p1}=1.25$.

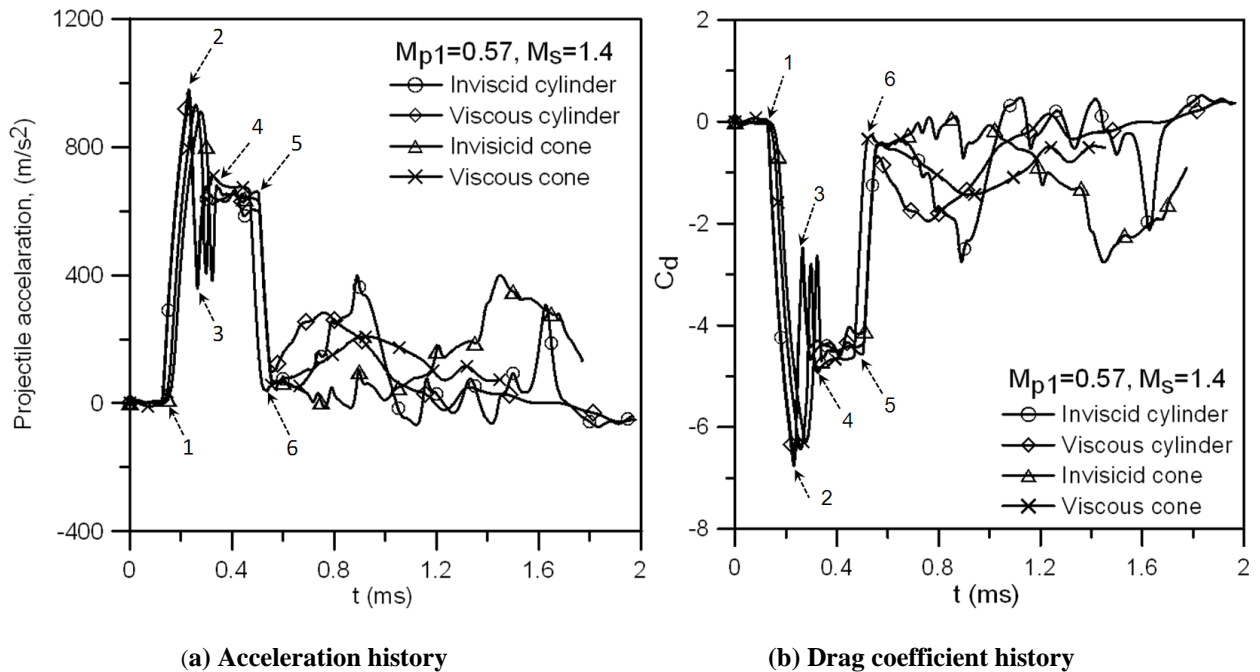


Figure 6: Acceleration and drag coefficient history of the cylindrical and conical projectile of inviscid and viscous simulation for Mach number $M_s=1.4$ and $M_{p1}=0.57$.

there is a fluctuation in the acceleration of the cylindrical projectile. This can be attributed to the formation of the bow shock wave in front of the cylindrical projectile⁹.

For the conical projectile, the fluctuation corresponds to the interaction with the secondary shock wave for state point c to d is not observed as seen from Fig. 4 and Fig. 3. This shows that the interaction between the projectile and the secondary shock in the case of cylindrical projectile is quite different from that of the conical projectile. This is due to the difference in the configuration and its effect on the flow field. This can be clearly observed later in Fig. 10b and 10c where the contours of the projectile Mach numbers are plotted. The smooth interaction between the conical projectile and the secondary shock wave reveals that the excursion of waves does not occur during the formation of bow shock wave, as in the case of a cylindrical projectile⁶. From the state e onwards, the projectile undergoes a steady deceleration. This is due to the reason that the driving force from the jet diminishes as the projectile moved away from the launch tube exit. It can also be observed that the cylindrical projectile decelerates faster than the conical projectile.

In order to investigate the projectile aerodynamic characteristics, the drag coefficient history of the cylindrical and conical projectiles are computed, where the drag coefficient is defined in Rajesh et al.⁹ The drag coefficient histories show the same trend as that of the acceleration histories as shown in Figures 4b 3b 5b 6b, where the acceleration and drag coefficient histories are plotted for various projectile Mach numbers.

At the state a, the front face of the projectile starts interacting with the under expanded jet results in pressure difference in the either side of the projectile. The drag on the projectile is negative till the state point b, where the projectile interacts with the secondary shock wave. Till this state, both the cylindrical and conical projectile have similar drag coefficient. This revealed that the configuration has no effect on the aerodynamic characteristics of the projectile. At state b, the drag coefficient becomes positive. From the state c to d, the fluctuation in the drag coefficient of the cylindrical projectile is observed and it is not seen for the conical projectile. From the state e onwards, the drag coefficient of the conical projectile is significantly less than that of the cylindrical projectile, as shown in the Fig. 3. This verifies the fact that the strength of the bow shock wave being developed in front of the conical projectile is weaker than that of the cylindrical projectile.

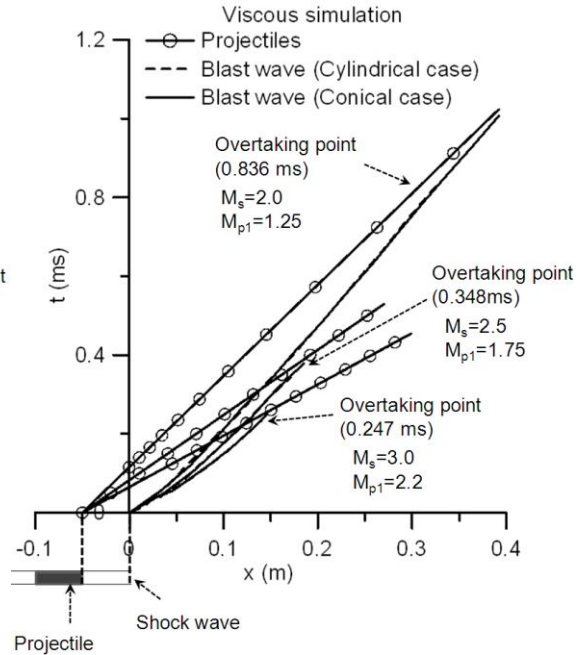
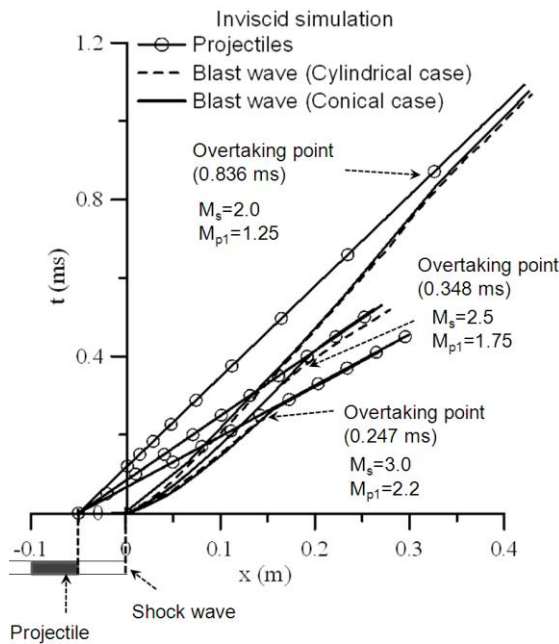
During the projectile overtaking the blast wave, the bow shock wave interacts with the blast wave and forms the familiar triple point on the either side of the projectile. This overtaking phenomenon corresponds to state g in Fig. 3 where the fluctuation in the drag of the projectile is very small. This is due to the attenuation of the blast wave to an

extent where the pressure jump across the wave is quite lesser than that needed to create a drastic fluctuation in the aerodynamic characteristics of the projectile. This reminds the possible overtaking conditions proposed by watanabe8 that the projectile can undergo either supersonic overtaking or the subsonic overtaking based on the projectile Mach number relative to the flow behind the blast wave. But in real situations, the blast wave strength is diminishing rapidly that alters the flow conditions behind the blast wave and makes the only possible overtaking condition to be supersonic. One thing that is being observed in the present computations is that the overtaking phenomenon affects the aerodynamic characteristics of the projectile only for larger Mach numbers. It can be shown for the case of $M_s=3.0$, the effect of overtaking the blast wave on aerodynamic characteristics is observed as a fluctuation in the drag coefficient of the projectile whereas for the smaller Mach numbers, this fluctuation is not observed and it is negligible. Thus, for the lower Mach numbers, the unsteady flow structures determine the aerodynamics of the projectile rather than the overtaking phenomenon.

One more interesting thing observed is the interaction of the projectile with the secondary shock wave. When the projectile passes through the secondary shock wave, the relative projectile Mach number increases to the supersonic state. It is noticed that during the projectile-secondary shock wave interaction, the dynamics of the shock wave depends on the configuration of the projectile. This can be clearly seen from the Fig. 3 and 4, for the case of cylindrical projectile, the shock wave preserves its shape till the interaction. But for the conical projectile, the characteristics of the secondary shock wave change as it is approached by the conical face of the projectile. This is mainly due to the turning of the flow field in the vicinity of the conical face of the projectile. This causes the normal shock wave to evolve as an oblique shock wave to meet the downstream flow conditions.

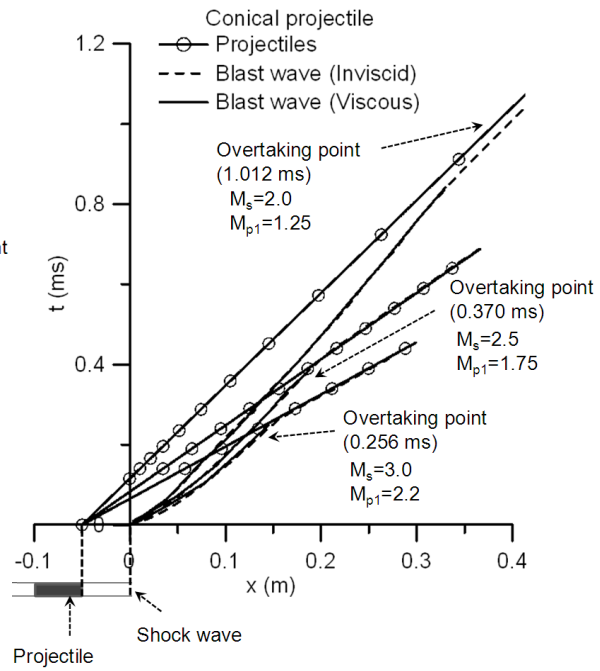
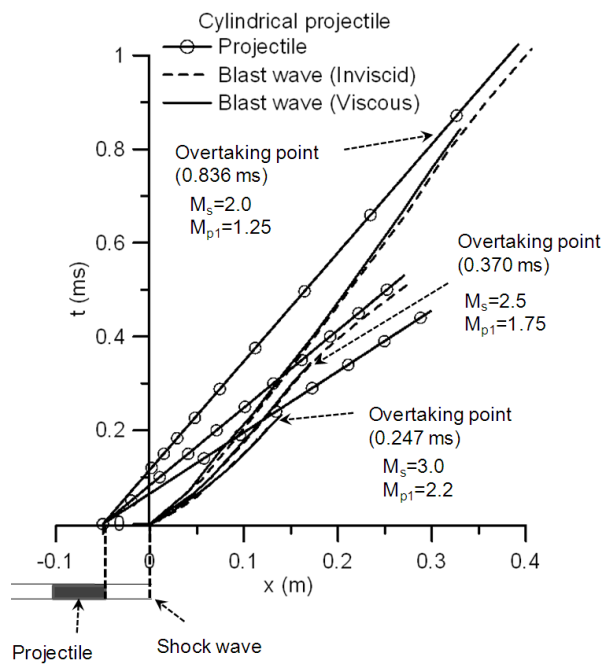
To identify the projectile motion, blast wave motion and the overtaking process, the $x - t$ diagram is shown in Fig. 7. The blast wave starts from the launch tube exit and the projectile starts at 50 mm behind the shock wave. As the time progresses, the paths of the projectile and blast wave are converging and coming close to each other. The point where the path of the projectile meets the path of the blast wave is identified as the overtaking point and is shown in the figures. It is noted that the path of the blast wave and path of cylindrical projectile never meet at a specific point. This is because of the detached bow shock wave standing in front of the cylindrical projectile with some shock standoff distance. In the case of the cone, the shock wave formed in front of the projectile can be attached or detached depending on the critical Mach number M_{cr} and the projectile cone angle θ_{max} . Below the critical Mach number M_{cr} , the shock wave is detached. Even at low projectile mach numbers the shock stand-off

distance for the cone is much smaller compared to that of the cylindrical projectile. So the overtaking point is considered as the point where the shock wave formed in front of the projectile starts merging with the precursor shock wave.



(a) Inviscid simulation, Effect of projectile configuration

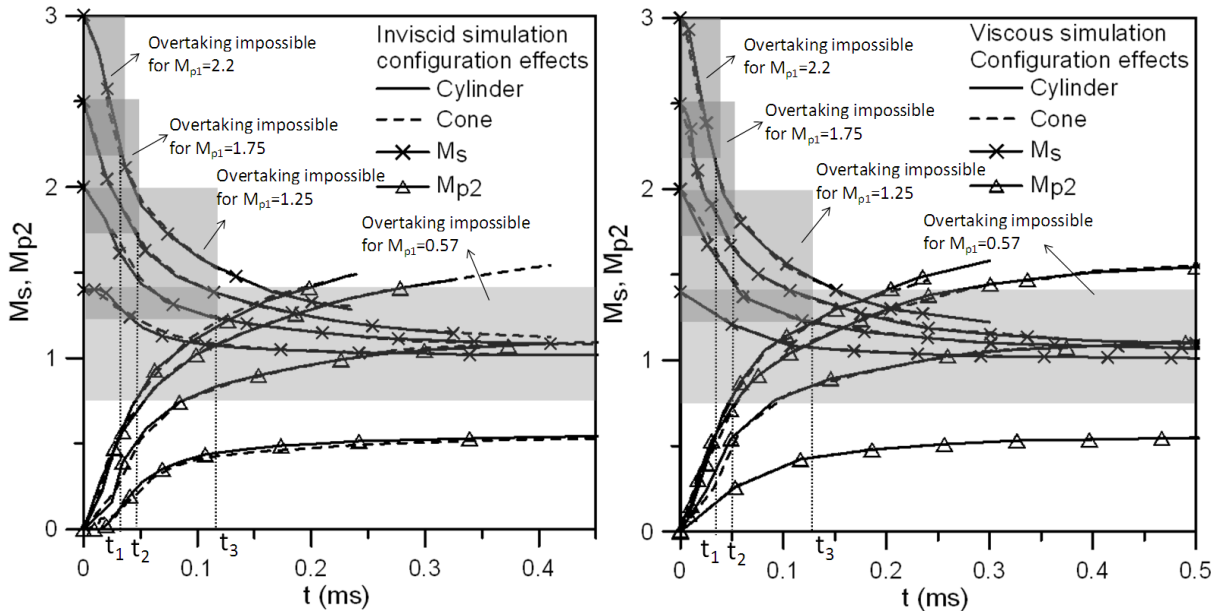
(b) Viscous simulation, Effect of projectile configuration



(c) Cylindrical projectile, Effect of viscosity

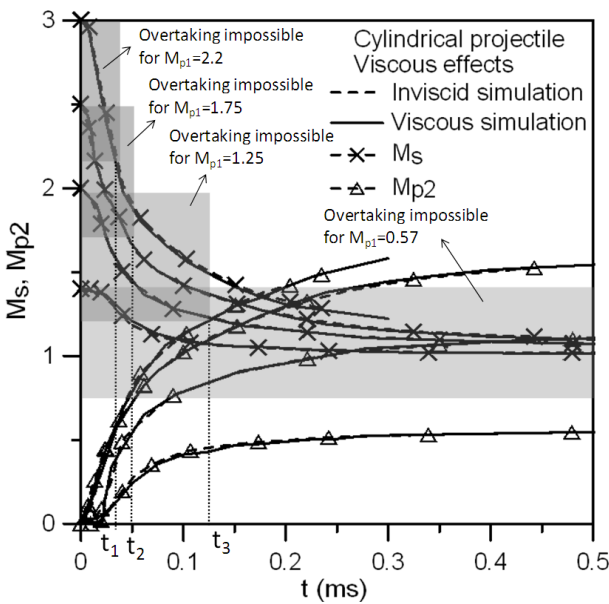
(d) Conical projectile, Effect of viscosity

Figure 7: $x-t$ diagram of the projectile and blast wave

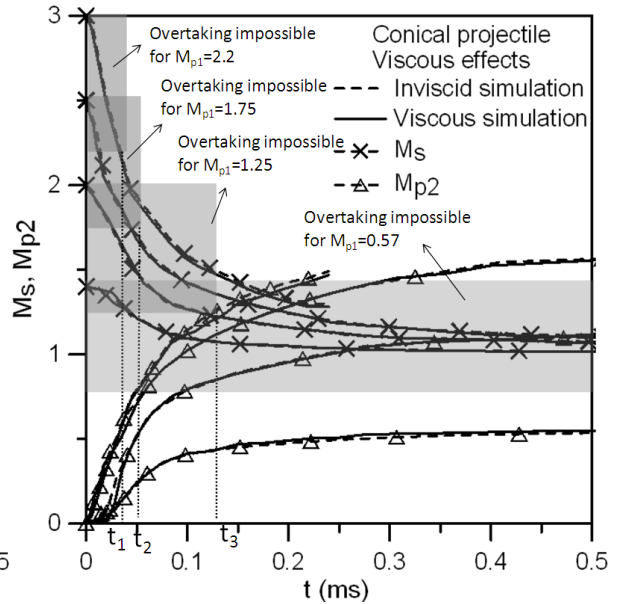


(a) Effect of the configuration, for Inviscid simulation

(b) Effect of the configuration, for viscous simulation



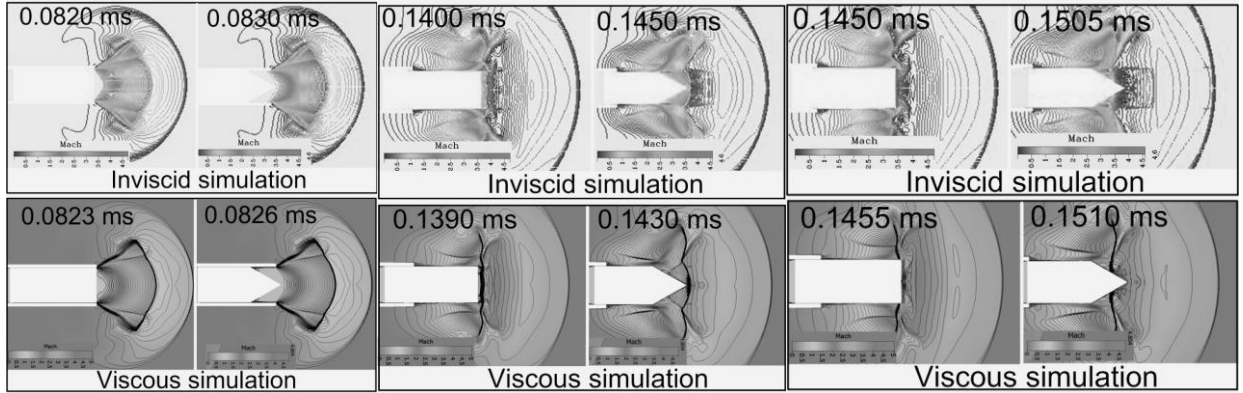
(c) Effect of viscosity, for cylindrical projectile



(d) Effect of viscosity, for conical projectile

Figure 8: variation of M_s and M_{p2} with respect to time

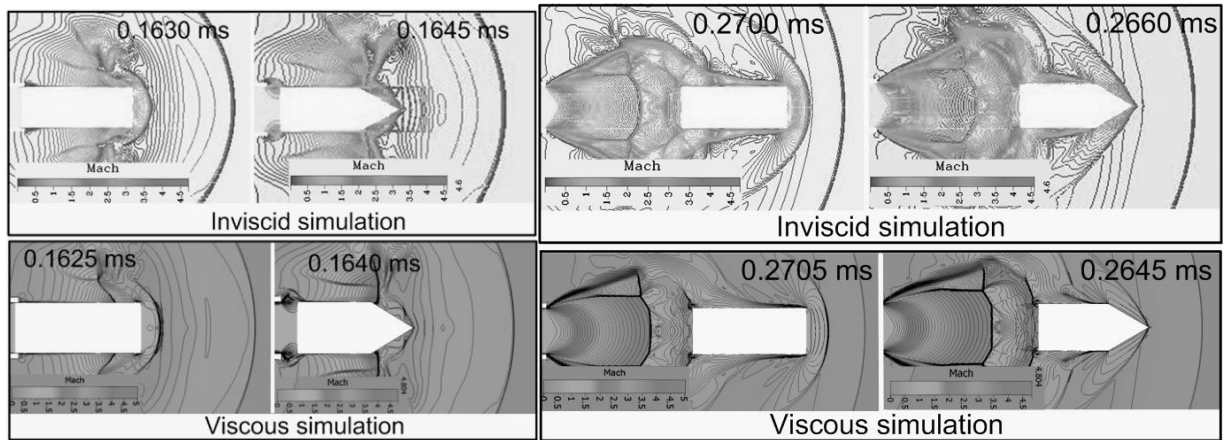
The effect of configuration on overtaking phenomena is investigated for both inviscid and viscous case. From the figure 6a and 6b, it is clear that the configuration does not affect the overtaking path except that the bow shock wave standoff distance for the cylinder is much larger than that of the cone. Because of this, the overtaking time for the cone seems to be more than that of the cylinder.



(a)

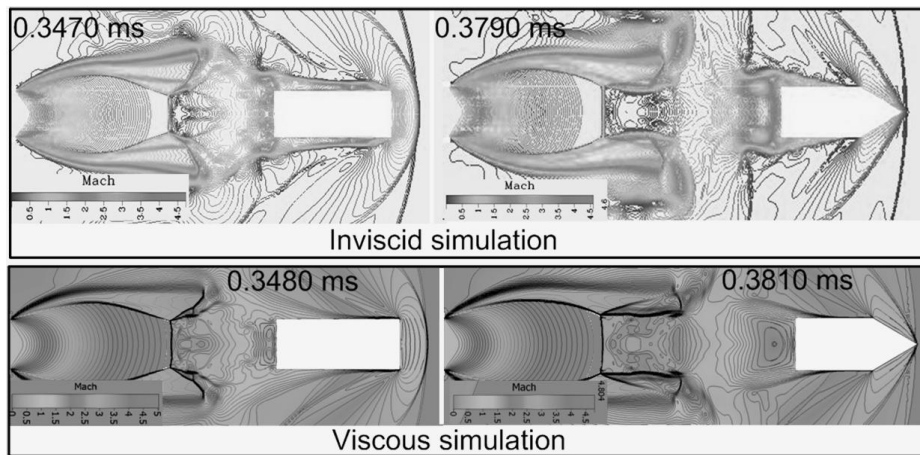
(b)

(c)



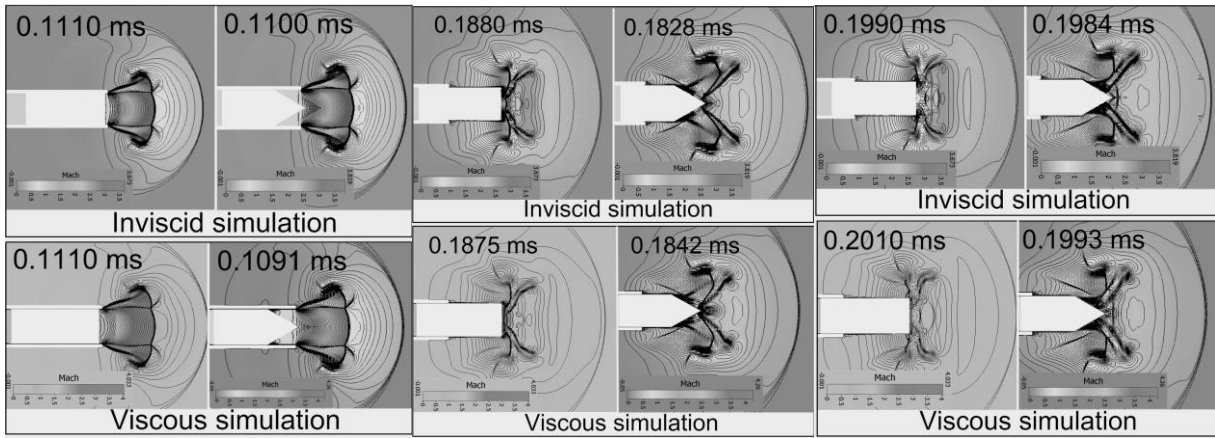
(d)

(e)



(f)

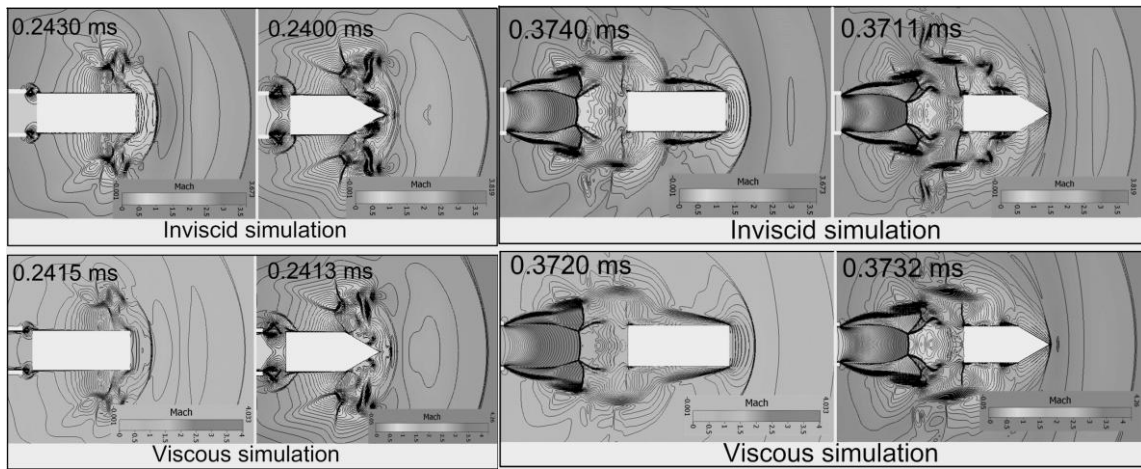
Figure 9: Mach contours of the cylindrical projectile for $M_{PI}=1.75$ and $M_s=2.5$



(a)

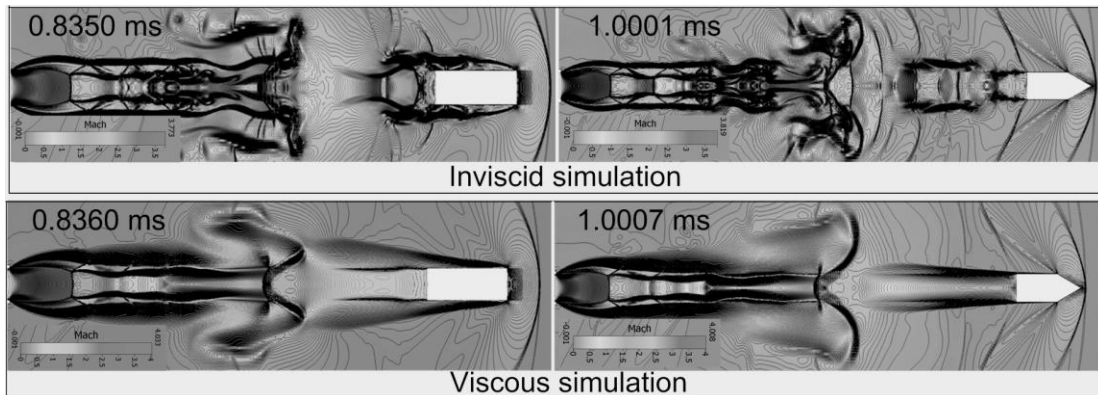
(b)

(c)



(d)

(e)



(f)

Figure 10: Mach contours obtained for $M_{p1}=1.25$ and $M_s=2$.

To get the possible overtaking regimes of the projectile at various mach numbers M_s and M_{p2} is plotted in Fig. 8. It clarifies the effect of the attenuating blast wave on the overtaking process. It can be seen that during the whole

overtaking process, the blast wave Mach number is varying from an impossible overtaking ($M_{pl} < M_s$) condition to possible one ($M_{pl} > M_s$)⁹. The overtaking is impossible until time t_1 for the case of $M_{pl}=3$ and time t_2 for the case of $M_{pl}=2.5$, since the blast wave travels faster than the projectile in this regime, and after this time the overtaking becomes possible due to the blast wave attenuation⁹.

III.B. Viscous effects

The Fig. 10 shows the flow structures, mainly the shock wave structures, for cylindrical and conical projectile for both the inviscid and viscous case. It is clear that the shock structures are different for inviscid and viscous case for the distance far away from the launch tube. This can be regarded as the effect of viscosity. Though the viscous effect cannot make the shock structure to disappear³, the overall flow field and the shock structures of the viscous simulation is different from that of the inviscid case. This is because of the fact that the viscosity alters the flow structures mainly by means of thickening the shear layers near the lip region of the launch tube. This thickening and diffusion of the shear layer do not occur in inviscid flows.

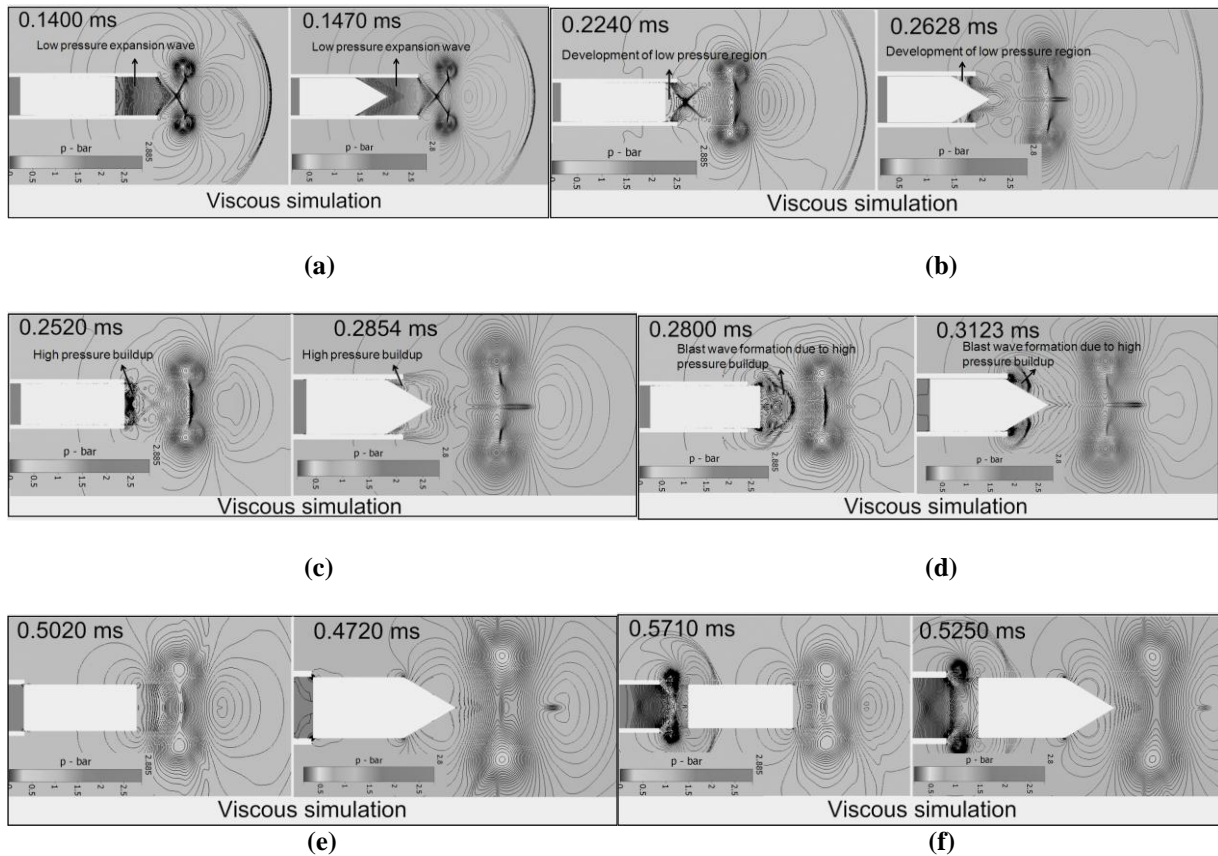


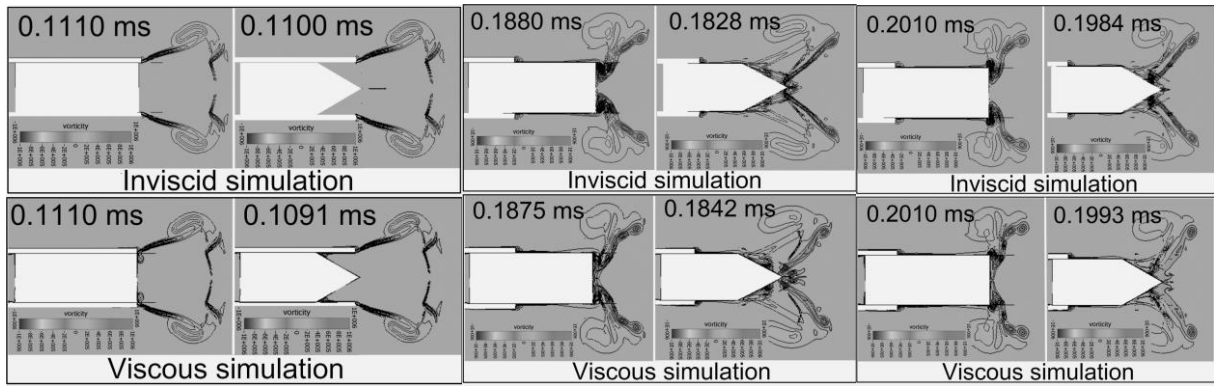
Figure 11: Pressure contours of viscous simulation obtained for $M_{pI}=0.57$ and $M_s=1.4$

The diffusion of the shear layer later causes drastic changes in the shock structures for viscous case. The viscosity does not affect the shock structures but it affects the shear layers and slip lines and it is responsible for the changes in the shock wave structures away from the launch tube. The underlying basic flow structures for the inviscid and the viscous case is similar. But because of the viscous effects the evolution of the flow structures for the viscous case is different from that of the inviscid case. The distinct shear layer is seen in the Fig. 10 for the inviscid case is not seen for the viscous case. This is mainly because of the role of the viscosity on thickening the shear layer drastically and affects the flow field.

III.C. Vorticity contours at $M_s=2.0$ and $M_{p1}=1.25$

The very interesting feature of the viscous flow is the diffusion of the vorticity. In order to bring out the effect of viscosity on the flow structures clearly, the vorticity contours are obtained. It is observed that the viscous effect is a dominating factor in determining the structure of the slip lines. Fig. 12 shows the effect of the viscosity in diffusion of the vorticity at various instants of time. From Fig. 12, the slip lines that are formed at the launch tube exit are clearly seen where there is a velocity discontinuity across them. From Fig. 12a to Fig. 12d, the evolution of the slip lines seems to happen in the similar fashion for both the inviscid and viscous cases. This is because the diffusion process happens at slower rate than the whole process. As the time progresses, the evolution of the flow structures show that the diffusion of the vorticity dominates the process. The flow structure of the viscous case becomes different from that of the inviscid case at later stages. Similar behavior is observed when considering the viscous effects on the flow structures around the moving projectiles. The shear layer originates from the sharp corner of the cylindrical projectile. Beneath the shear layer the complicated shock structures are seen for the inviscid case near the body. But for the viscous case, the structure of the shear layer gets affected by the viscosity and its diffusion is clearly seen. This may be responsible for the absence of the shock structures near the wall of the projectile.

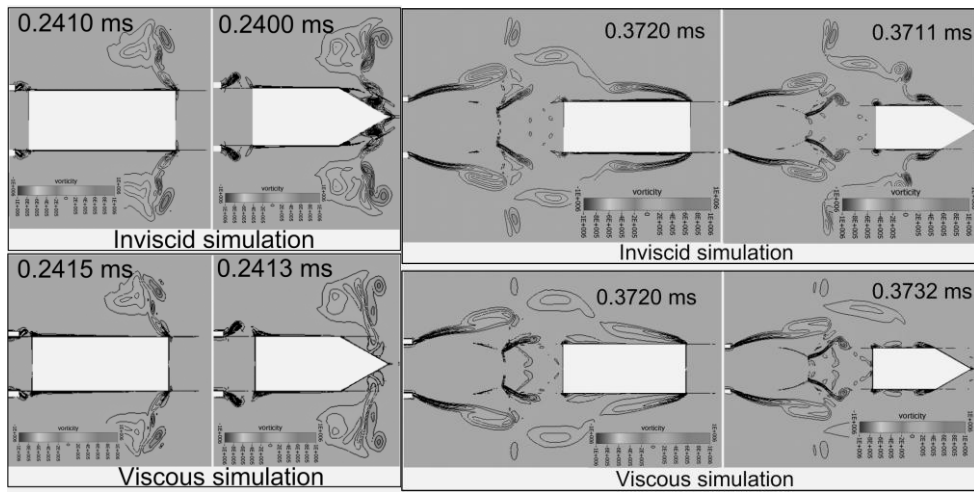
When considering the aerodynamic drag of the moving projectile, the viscosity plays a significant role. The boundary layer forms over the walls of the projectile that are responsible for the shear or viscous drag which are absent in the case of inviscid flow. Since the pressure drag is considered to be the dominant one and the effect of viscosity on the total drag is negligible. This effect of viscous drag can be seen in the C_d of the projectile from the Figures. 4b, 3b, 5b and 6b. There are some interesting phenomena like shock-boundary layer interaction takes place in viscous flow near the wall of the moving projectile.



(a)

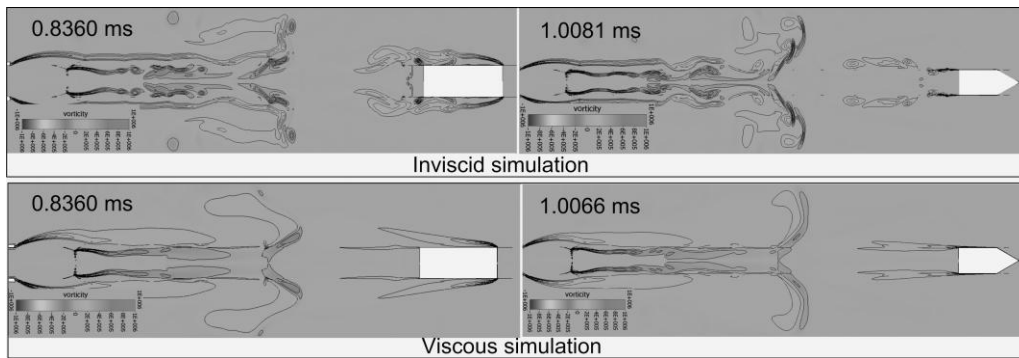
(b)

(c)



(d)

(e)



(f)

Figure 12: Vorticity contours obtained for $M_{P1}=1.25$ and $M_s=2$.

III.D. Flow structures for $M_{pl}=0.57$ and $M_s=1.4$

The projectile flow field interaction in this case is entirely different from that of the previous cases. When the projectile travels inside the launch tube, the shock wave diffraction is followed by an under expanded subsonic jet. The jet is subsonic and hence the expansion wave can travel upstream inside the launch tube towards the projectile face and creates a low pressure in front of the projectile. This pressure difference causes the acceleration of the projectile and this is marked as state 1 in Fig. 6 and the corresponding pressure contours are shown in Fig. 11a.

There is a significant increase in the acceleration of the projectile till its front face coincides with the exit of the launch tube. When the projectile reaches the exit of the launch tube, a further low pressure creates locally near the front face of the projectile. Following the low pressure formation, a high pressure build up takes place in that region. This can be manifested as a wave like phenomena. The pressure builds up along with the forward motion of the projectile resulting in building up of high pressure in the front face of the projectile. The duration of this process is so short and there is a marked decrease in the acceleration of the projectile. This process takes place between state 2 to state 3 as shown in Fig. 6. The increase in the pressure in front of the projectile can be seen in the Fig. 11c. This high pressure is enough to create blast wave in front of the projectile. This blast wave travels forward and attenuates results in the increase in the pressure difference on the either side of the projectile. This process of formation of blast wave and its attenuation is clearly shown in Fig. 11c to 11d. There is a increase in the acceleration of the projectile from state 3 to state 4. From the state 4 onwards there is a uniform pressure in front of the projectile causes constant acceleration till the projectile exits from the launch tube and this process is marked from state 4 to state 5. Once the projectile exits from the launch tube, the formation of secondary blast wave takes place and it sweeps over the surface of the projectile followed by the formation of low pressure in the rear face of the projectile. This causes the projectile to decrease in the acceleration in a short duration of time from state 5 to state 6. Till the state 6, both the projectile follows the same trend in the acceleration of the projectile for both the viscous and inviscid simulation as seen from Fig. 6. The drag coefficient of the projectile shows the similar trend as that of the acceleration of the projectile. From the state 6 onwards, there are complex interaction among the projectile and the flow-field that are unique for the projectile configuration and for the inviscid and viscous simulation.

IV. Conclusion

A computational study was performed using moving grid method to analyze the effect of projectile configuration on the overtaking process in a blast flow field. Both inviscid and viscous simulations have been carried out to analyze the flow field. The study shows that the aerodynamic characteristics of both the projectile configurations are unaffected during the overtaking process as they undergo only supersonic overtaking in low blast wave Mach number conditions. The projectile configuration may have deterministic effects on the aerodynamic characteristics of the projectile during the overtaking process at higher mach numbers. However, the projectile configurations do affect the aerodynamic characteristics, when it travels in the unsteady flow field prior to overtaking, especially when it interacts with the secondary shock wave behind the primary blast wave. It is observed from the viscous simulation that the viscosity does not affect the aerodynamic characteristics of the projectile but it does affect the flow field structures. The main role of viscosity on vorticity diffusion alters the shock wave structure of the flow field.

References

- [1]. R.Hillier., Computation of shock wave diffraction at a ninety degree convex edge, Shock waves, vol. 1, 1991, pp- 89-98.
- [2]. Sun.M, Takayama.K., Vorticity production in shock diffraction, Journal of Fluid Mechanics, vol 478, 2003, pp- 237-256.
- [3]. Sun.M, Takayama.K., The formation of a secondary shock wave behind a shock wave diffracting at a convex corner, Shock Waves, vol. 7, No. 5, 1997, pp- 287-295.
- [4]. Rajesh.G, Kim.H.D, Matsuo and Setoguchi.T., A study of the unsteady projectile aerodynamics using a moving coordinate method, IMechE, Vol 221, 2007.
- [5]. Martin Brouillette., Ritchmyer-Meshkov instability, Annu.Rev. Fluid Mech. 2002. 34:445-468.
- [6]. Z.Jiang, K.Takayama, and B.W.Skews., Numerical study on blast flow fields induced by supersonic projectiles discharged from shock tubes. Phys.Fluids, vol.10, No.1, 1998, pp.277-288.
- [7]. Z.jiang.,Wave dynamic processes induced by a supersonic projectile discharging from a shock tube. phys.Fluids, vol.15, N0.6, 2003, pp. 1665-1775.
- [8]. Watanabe,R., Fujii,K., and Higashino,F., Numerical solutions of the flow around a projectile passing through a shock wave, AIAA paper 95-1790, 1995.
- [9]. Rajesh.G, Kim.H.D, Setoguchi.T., Projectile Aerodynamics Overtaking a Shock Wave. J. Spacecraft and Rockets, Vol.45, No.6, 2008.
- [10].A.E.Bryson and R.W.F.Gross., Diffraction of strong shocks by cones, cylinders and spheres, J. Fluid. Mech, vol 10, issue 01, pp-1-16, 1960.
- [11].Whitham. G.B, A new approach to problems ofshock dynamics part 2. Three dimensional problem, J. Fluid. Mech, vol 10, issue 01, pp-1-16, 1960.

[12].Ahmadakia.H and Shirani.E., Transonic and supersonic overtaking of a projectile preceding a shock wave, JAST, vol 2, No. 4, pp 45-53, 2005.

[13].CFD FASTRAN Theory Manual Version 2010.